2014 Canada-China Conference on Advanced Reactor Development(CCCARD-2014)
Niagara Falls Marriott Fallsview Hotel & Spa, Niagara Falls, Ontario Canada, April 27-30, 2014.

CCCARD2014-xxx

A COMPUTATIONAL BENCHMARK STUDY OF FORCED CONVECTIVE HEAT TRANSFER TO WATER AT SUPERCRITICAL PRESSURE FLOWING WITHIN A 7 ROD BUNDLE

D. McClure[1], A. Rashkovan[1] and D.R. Novog[1]
[1] McMaster University, Hamilton, Ontario, Canada

Abstract

A methodology for computational fluid dynamics (CFD) simulations was developed for the submission to the Japan Atomic Energy Agency (JAEA) computational benchmark exercise related to supercritical water heat transfer in rod bundles. The experiments conducted by the JAEA are those of upward flow of supercritical pressure water in a 7 rod bundle; of which there is an (i) isothermal case, (ii) a low enthalpy and low heat flux case and (iii) a high enthalpy and high heat flux case. Given the complexity of the geometry and flow conditions a thorough separate effects study was performed examining all modelling options. Through these studies the optimal turbulence model and mesh parameters were selected. The paper concludes with a discussion of the future work required to finalize the submission.

1. Introduction

The supercritical water reactor (SCWR) is one of the multiple innovative reactor designs that have been recognized by the Generation IV International Forum (GIF). Canada and China have both chosen to contribute to the research and development efforts involved in the conception of the SCWR. The SCWR will utilize a steam cycle which operates above the critical pressure for water (22.1 MPa). A distinct improvement is the impossibility of a critical heat flux scenario. Instead, the thermal-hydraulic design focus is upon what is known as deteriorated heat transfer (DHT), which can occur when buoyancy or streamwise acceleration effects are appreciable.

The regimes of heat transfer to supercritical pressure fluids are very much different than that of heat transfer to subcritical pressure fluids. Pioro and Duffrey [1] performed a very thorough review of the experiments of heat transfer to supercritical pressure water. Three regimes of heat transfer were identified to be; Enhanced Heat Transfer (EHT), Normal Heat Transfer (NHT) and Deteriorated Heat Transfer (DHT). The regime of NHT can be predicted using various forms of the Dittus-Boelter correlation, whereas the regimes of EHT and DHT require correlations catered specifically to flows of supercritical pressure fluids and are not predicted well by traditional empirical correlations.

The manner in which the physical properties of supercritical fluids vary as a function of temperature contributes to the unique heat transfer regimes. As the temperature increases from below the pseudocritical temperature, Tpc – which is defined as the temperature at which the specific heat capacity of the supercritical fluid reaches a maximum – the specific heat capacity

goes through a sharp maximum while density, dynamic viscosity, and thermal conductivity decrease abruptly as Tpc is crossed. This behaviour is shown in Figure 1.

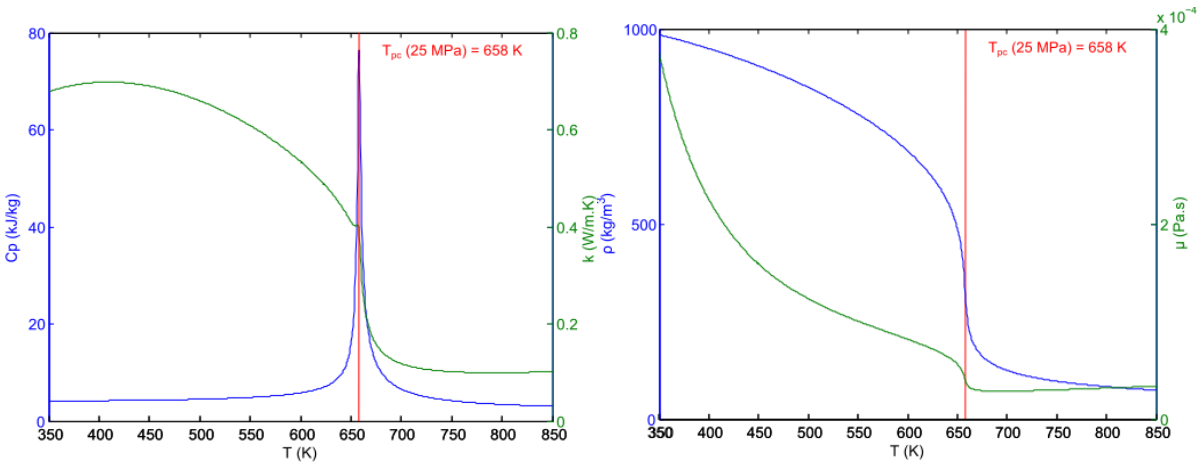

Figure 1 The physical property variation of water at *25 MPa*

Effects of streamwise acceleration as well as buoyancy have been considered in contributing to DHT. The Kv parameter of Moretti et al [2] and the Bo* parameter of Mikielewicz [3] give thresholds for the importance of streamwise acceleration and buoyancy effect, respectively.

The experiments planned for the JAEA computational benchmark exercise are expected to lie away from regions where buoyancy and streamwise acceleration are deemed significant. Any departure from NHT is expected to be due to the unique property variation of supercritical fluids near Tpc. The EHT regime can be explained by considering three effects. As the wall temperature reaches Tpc the thermal conductivity decreases, the specific heat increases and the dynamic viscosity decreases. Although the decrease in thermal conductivity will impair heat transfer, this is more than compensated by the large specific heat and the low viscosity which acts to thin the viscous sublayer. As the heat flux increases, this enhancement of heat transfer diminishes since the region of large specific heat decreases in size due to the large temperature gradients present with larger heat flux [4].

A very illuminating set of experimental data within the EHT regime is that of Yamagata et al [5]. They performed experiments with supercritical water flowing in tubes in conditions that avoided DHT. They found that as the bulk temperature nears Tpc the heat transfer becomes greatly improved and the peak in the heat transfer coefficient (HTC) is located at a bulk temperature slightly less than Tpc. The peak in HTC is seen to decrease as the heat flux is increased. The experimental data of Yamagata et al [5] has been used extensively to validate computational approaches [6-9].

The shear-stress transport (SST) turbulence model [10] has been used by multiple authors and has demonstrated its strength in predicting wall temperature distributions across multiple heat transfer regimes for supercritical fluid flows. Yu Zhu [11] offered a thorough comparison of the predictive capabilities of SST versus that of RNG k-ϵ [12]. Zhu chose multiple validation cases and SST was chosen as superior. Zhu also determined that a $y+ < 0.1$ was to be used in

order to achieve a mesh independent solution. The work of Palko et al [13] showed the success of SST in predicting wall temperature distributions in tubes across multiple heat transfer regimes. A low coolant and a high coolant flow case were chosen to demonstrate this. A $y+ < 1$ was determined, in this case, to give mesh independent results.

The vast majority of experiments for heat transfer to supercritical fluids have been performed in tubes. Therefore, there exists a very limited dataset of which to compare computations of flows in complex geometries such as bundle flow. This is somewhat resolved by studying subcritical bundle flows. Trupp et al [14] studied isothermal flow in a simulated "infinite" rod bundle with various pitch to diameter ratios at various Reynolds numbers and made measurements of mean axial velocities, local wall shear stress and five of the six Re stresses. Trupp et al [14] deduced the magnitude and distribution of the secondary flows from the mean velocity data. Their results showed anisotropy in the turbulence as well as a small but appreciable secondary flow. Both of these phenomena increase the shear stress at the wall and therefore have an enhancing effect on heat transfer.

The JAEA Computational Benchmark Exercise is being carried out by multiple research groups around the world in an effort to improve the knowledge base of modelling heat transfer to supercritical fluids. Following the submission of the final results a journal paper will be produced by the organizing committee that highlights successful as well as unsuccessful modelling approaches with consideration of turbulence model choice and mesh choice (including near wall resolution and control volume geometry (hexahedral vs. tetrahedral)). This paper documents the separate effects study which will be used to determine the modelling, geometry and mesh options for the McMaster University final submissions.

2. JAEA Experimental and Modelled Conditions

The experiments conducted by the JAEA were done in upward flow in a 7 rod bundle which was electrically heated. The simulated fuel rod contained a heating element which was encased in Boron Nitride; this was then contained within a cladding of Inconel 600. Thermocouples were set into the cladding at various azimuthal positions for each rod at various axial positions. The entire heated length of the test section was 1.5m with grid spacers of 0.025m length staggered axially along the section. The modelled geometry is shown for clarity in Figure 2, while a full description is available in [15].

2.1 Modelled Geometry

Figure 2 (a) shows the rod bundle within a shroud and Figure 2 (b) shows the grid spacer which holds the rods in place at various positions along the test section. Each rod has a diameter of 8mm and the closest spacing between the rods is 1mm, giving a pitch to diameter ratio of 1.125. In total there are six grid spacers, with five of them positioned within the heated section and one positioned upstream of the heated section.

Figure 2 (b) shows the complex features of the grid spacer, which include the bars (similar to positioning buttons in the interior of PWR spacer grids) that span the length of the spacer and

are oriented such that they are pitched off the flow direction axis in order to enhance mixing within and downstream of the grid spacer.

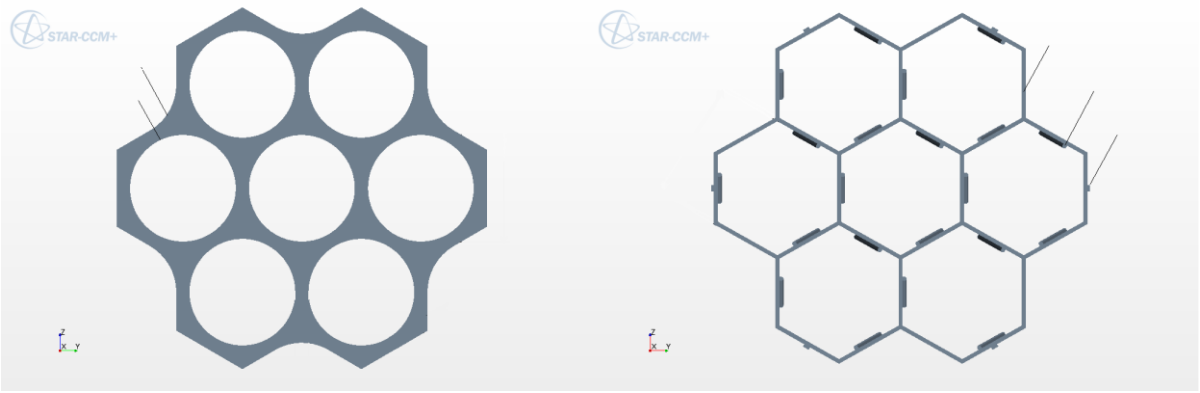

Figure 2 (a) Rod bundle and (b) Grid spacer geometry

2.2 JAEA Experimental Conditions

The experiments to be studied in the benchmark include 1 isothermal and 2 heated cases as outlined in the following tables.

Case	Inlet Temperature (K)	Inlet Pressure (MPa)	Mass Flux (kg/m^2s)
A1	297.35	25.0	2283.44

Table 1 Isothermal experimental condition

Case	Inlet Temperature (K)	Inlet Pressure (MPa)	Mass Flux (kg/m^2s)	Heater A (kW)	Heater B, D, F (kW)	Heater C, E, G (kW)
B1	353.58	24.98	1447.56	19.67	22.51	22.52
B2	519.58	25.03	1432.97	34.14	34.08	34.13

Table 2 Heated experimental conditions

3. Computational Procedures and Modelling Considerations

The commercial software package STAR-CCM+ 8.06.005 was used to mesh and model each of the separate effects to be summarized in Section 4.1 and will be used to mesh and model the experimental conditions seen in Tables 1 and 2.

3.1 Turbulence Modelling

Turbulence models used within this study were limited to the Reynolds Averaged Navier Stokes (RANS) type. There are two types of turbulence models within the RANS approach;

eddy viscosity models (EVM) of which the SST model is an example and Reynolds Stress models (RSM) of which the model suggested by Launder et al [16] is most commonly used.

EVMs are based on the Boussinesq approximation in which the Reynolds stress tensor is calculated as a linear function of the velocity gradient tensor multiplied by the scalar eddy viscosity; much like the way viscous stress is related to the velocity gradient tensor by a molecular viscosity. This approach requires the solution of the conservation equations as well as two additional transport equations of turbulence. The eddy viscosity is then defined in terms of these turbulence parameters.

A step up in complexity from the EVM is the RSM. Instead of the Boussinesq approximation being used to simplify the calculation of the Reynolds stress tensor, a transport equation is derived for each of the six Reynolds stresses which cast them in terms of the mean velocity field. In addition to these transport equations, an equation for ϵ is solved. This leaves the RSM with seven transport equations to solve in addition to the conservation equations.

The computational cost of the RSM is certainly higher. Furthermore, the highly coupled nature of the Reynolds stress transport equations lead to convergence issues that result in many more iterations required as compared to the EVMs. As opposed to EVM models, the RSM does allow for the prediction of the anisotropic nature of the turbulent field, and streamwise curvature as well as the resolution of secondary flows.

Models of both types have been used in order to investigate the various flow and heat transfer phenomena present within the JAEA experiments.

3.2 Mesh Sensitivity

The importance of obtaining mesh independent results cannot be overstated, especially for the case of heat transfer to supercritical water due to the very thin laminar sublayer in such flows. The resolution of the heated surface boundary layer is of utmost importance due to the large variation in thermophysical properties with temperature. In each of the separate effects studies described below mesh sensitivity studies were performed to ensure the discretization error was minimized to an acceptable level by systematically altering (i) the y+ value, (ii) the cell volume size in the bulk flow as well as (iii) the discretization in the axial direction.

3.3 CFD Methodology

The approach to modelling a complex flow geometry using CFD involves separating physical phenomena and verifying/validating a computational approach for each one. This procedure includes identifying the proper spatial and temporal discretization, the boundary and initial conditions to be used and, most importantly, the turbulence model that is capable of resolving key physical features of the flow deemed important by the CFD analyst. These studies are called Separate Effects Studies and following their completion the approaches found to be successful for each separate effects study are compared and a final computational approach is chosen to model the full geometry.

4. Computational Results

In the case of the JAEA benchmark exercise, several separate effects studies have been performed in order to choose the optimal turbulence model and discretization to employ for the final submission.

4.1 Separate Effects Studies

Study	Purpose	Key Result
Melling et al [17] validation	To assess various turbulence models in predicting Prandtl's secondary flow of the second kind and anisotropic turbulence in a square duct geometry	• EVMs incapable of resolving turbulence field and the secondary flow • RSM was found to predict the secondary flow and the anisotropic turbulence
Trupp et al [14] validation	To assess the capability of various turbulence models in predicting local wall shear stress, secondary flow and anisotropic turbulence in a rod bundle geometry	• RSM was able to predict the friction velocity and the anisotropic turbulence • SST was unable to resolve the turbulent field, its prediction of friction velocity was close to experiment
Yamagata et al [5] validation	To assess the capability of the SST and RSM turbulence models in predicting the heat transfer coefficient for supercritical water flowing upward in tubes	• SST and RSM were found to be successful in predicting the HTC

Table 3 Summary of each separate effect study and its key result

4.1.1 Melling et al [17] validation

The experiments of Melling et al [17] analysed near fully developed, isothermal flow in one quadrant of a duct of square cross section. All three mean velocity components and five of the six Reynolds stresses were measured and contour plots were produced of the mean velocity field and the turbulent field. The secondary flow vortices generated in the corners of the duct were found to be not much larger than 1% of the bulk streamwise velocity.

Calculations using RSM and various EVMs were completed using a mesh that gave $y+ < 4.5$. The magnitude of the streamwise velocity and the turbulent velocity are predicted fairly well by RSM. The secondary flow was underpredicted by RSM and the EVMs failed to predict any appreciable secondary flow. The orientation of the secondary flow is shown in Figure 3 (a) with the prediction of RSM in Figure 3 (b).

The reason RSM results are superior to EVM is due to their calculation of the Reynolds stress tensor. While RSM solves a transport equation for each Reynolds stress, EVMs rely on the

assumption (Boussinesq) that the Reynolds stress tensor is a linear function of the velocity gradient tensor. This, in general, is not true. As opposed to Prandtl's first type of secondary flow caused by e.g. flow passage curvature, Prandtl's second type of secondary flow has been shown to be caused by the anisotropy of the Reynolds stress [18] and without proper prediction of the Reynolds stress tensor secondary flows of this nature cannot be fully resolved. Therefore, it can be said that the resolution of the anisotropic nature of the turbulent field and secondary flow come hand in hand.

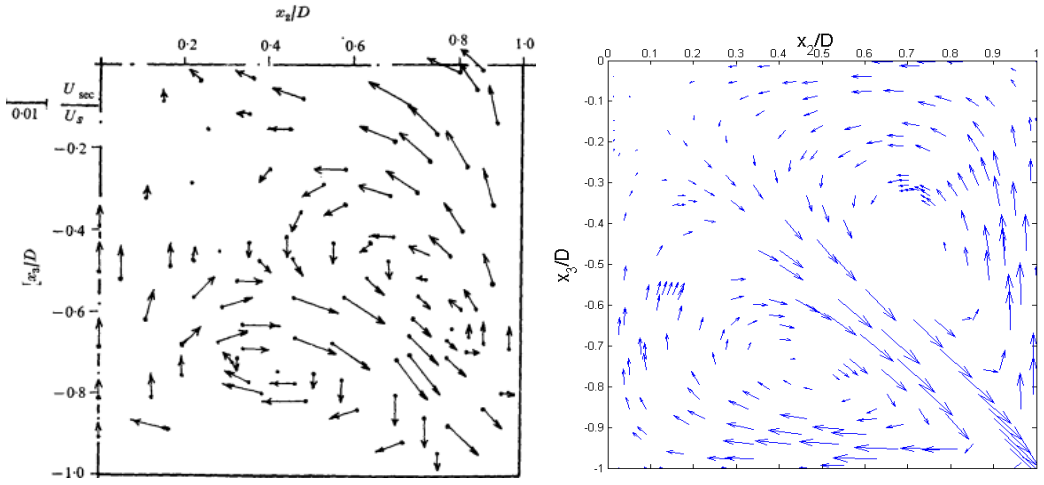

Figure 3 Distribution of secondary flow for (a) experiment (b) RSM

4.1.2 Trupp et al [14] validation

The experiments of Trupp et al [14] were done such that the experiment simulated an infinite bundle flow. Measurements of mean velocity, five of the six Reynolds stresses and local wall shear stress were made for one sixth of a subchannel. Experimental case C6 was used for comparison with calculations of which the experimental conditions are summarized in Table 4.

Test number	Pitch to Diameter Ratio	Reynolds number
C6	1.2	23760

Table 4 Experimental conditions of [14] chosen to be modelled

The computations were completed using a one sixth subchannel. Symmetry boundary conditions were used to accomplish this. A y+ < 0.7 was found to given mesh independent results. The turbulence models SST and RSM were used in this study.

RSM is shown to predict the turbulent velocities quite well for bundle flow as can be seen from Figure 4. Although only two plots are shown above, RSM had equal success at predicting all the turbulent velocities along the 0°, 15° and 30° axes. The 0° and 30° axes are the boundaries of the one sixth subchannel, where the 0° axis is the bisector of the two adjacent rod centres. Though the predictions of SST are not shown, they disagree substantially from experiment. The reason for this has been stated above in Section 4.1.1.

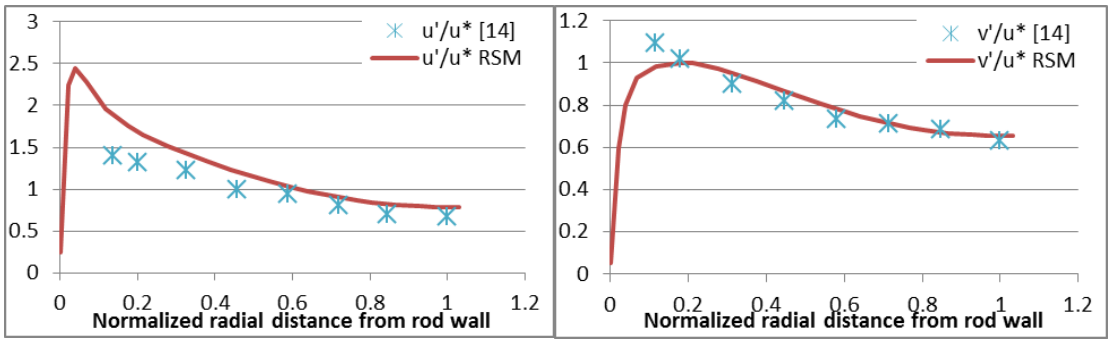

Figure 4 Comparisons of turbulent velocity normalized by friction velocity along the 30° axis

Model	u*, Friction Velocity (m/s)
C6 [14]	0.781
SST	0.720
RSM	0.740

Table 5 Comparison of average friction velocity

Despite SST's failure to reproduce the turbulent field seen in the experiment of [14], it was able to accurately predict the average friction velocity, u*. As friction velocity is an indirect measure of wall shear stress and wall shear stress is an extremely important factor in determining the HTC near a heated wall, this result gives some confidence in SST's ability to predict the HTC for bundle flows. However since these experiments did not measure heat transfer, this relationship can only be inferred.

4.1.3 Yamagata et al [5] validation

The experiments of Yamagata et al [5] were done for upward, downward and horizontal flow of supercritical water in a tube geometry. Measurements were taken of wall temperature for a variety of heat and mass fluxes. The case simulated is described in Table 6.

Flow Direction	Tube Diameter (mm)	Mass Flux (kg/m^2s)	Heat Flux (kW/m^2)
Up	7.5	1260	465

Table 6 Experimental conditions of [5] chosen to be modelled

The axisymmetry of the tube allowed the computations to be performed on a two dimensional axisymmetric mesh. The turbulence models SST and RSM were used in this study. In addition to comparing the predictive capability of the two turbulence models against the experimental data of Yamagata et al [5], it was determined that for $y+<1$ the HTC predictions remained sensitive. It was found that a $y+ < 0.15$ gave mesh independent results.

Figure 5 shows the relative success of both turbulence models in predicting the HTC within the EHT regime. As stated previously, Yamagata et al's [5] experimental conditions lie far away from regions of streamwise acceleration and buoyancy effects. Table 7 shows the threshold parameters of Mikielewicz [3] and Moretti et al [2] with the values of these parameters for Yamagata et al [5] and the cases of the JAEA.

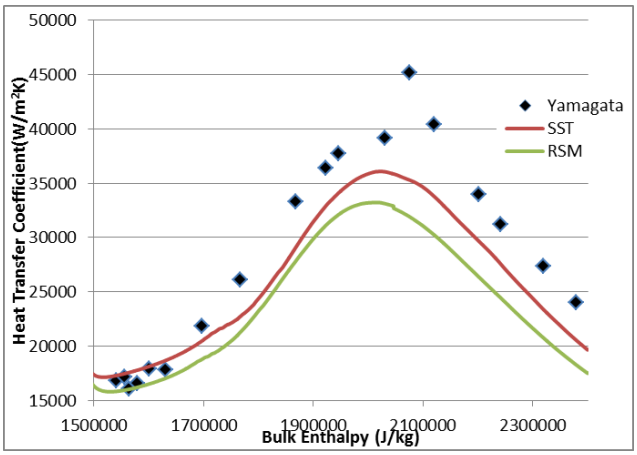

Figure 5 Comparison of HTC predictions to experimental data

Table 7 shows that the experimental conditions of Yamagata and the JAEA lay far away from regions of streamwise acceleration and buoyancy effects. This gives confidence that the validation case of Yamagata et al [5] has been the proper choice in determining a turbulence model that is able to resolve the heat transfer in the near wall region.

Parameter	**Yamagata**	**JAEA B1**	**JAEA B2**	**Threshold**
Bo*	1E-9 – 4E-8	1.4E-8 – 2.3E-8	6E-10 – 2.6E-8	> 6E-7 [3]
K_v	0.4E-9 – 1.2E-8	1E-8 – 1.6E-8	1.2E-8 – 3.2E-8	> 3.5E-6 [2]

Table 7 Threshold values to predict DHT

4.2 JAEA Geometry Computations

The results of the separate effects studies show the strength of RSM as well as SST. SST has been chosen as the turbulence model for the final submission for its cheaper computational cost, its lower residuals on convergence as well as its slightly improved prediction of HTC for supercritical water flow. As will be briefly discussed in this section, RSM showed difficulty in reaching convergence for the complex geometry of the JAEA test section. Based on this knowledge, the choice of SST will facilitate more trustworthy computations from a numerical point of view.

4.2.1 Heat transfer regime study

For the purpose of further supporting the SST selection for the benchmark experimental conditions, the 1/12th bundle geometry of the JAEA test section was simulated without any grid spacers. Many turbulence models were used and their results were expected to lie close to one another as these conditions are far away from buoyancy influence and streamwise acceleration. This is seen in the work of multiple authors [7,8,19] suggesting different turbulence models based on validation against Yamagata et al [5]. A sample of the results for the Case B2 experimental condition is shown in Figure 6. It is promising that each of turbulence model's predictions fall on top of each other. Due to convergence issues with RSM models on such a fine computational grid, RSM results are not available.

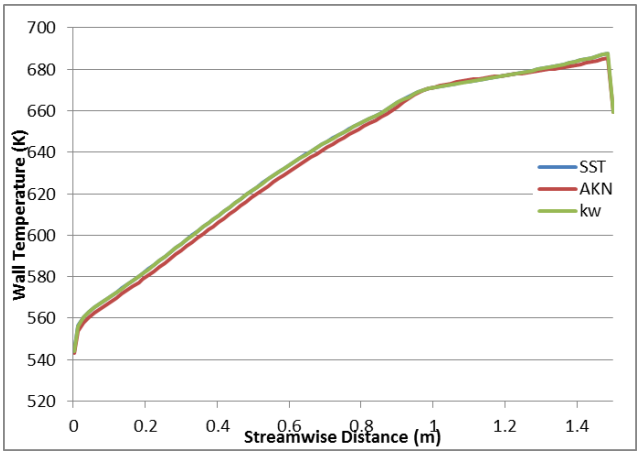

Figure 6 Wall temperature of the centre rod facing the subchannel in JAEA B2

4.2.2 SST's prediction bias and sensitivity

Prior to the final submission it is important to know where and to what extent the turbulence model choice will affect the predictions. It is also important to quantify the turbulence model's sensitivity to boundary conditions such as mass flux, heat flux and inlet enthalpy to ensure the model is giving stable predictions.

From the previous separate effects studies, SST has shown to fail to predict the turbulent field as well as secondary flows. SST did predict the frictional velocity reasonably well indicating that it may be capable of predicting bundle heat transfer. Regardless, SST is expected to struggle to capture the heat transfer enhancement caused by the grid spacer (since the turbulence caused by the structure is expected to have a high degree of anisotropy) and hence SST's prediction for the temperature field will not be as diffuse as experiment. An additional factor to consider is that because the geometry of the grid is complex, a high quality mesh is difficult to produce resulting in convergence difficulty for all turbulence models. Due to this, it has been determined that a tetrahedral mesh or a coarse hexahedral mesh must be used within and shortly downstream of the grid spacer. Both of these alternatives will result in increased diffusivity to the temperature and velocity field, thus providing a false diffusion that resembles the physical consequence of an anisotropic turbulent field and secondary flow.

4.2.3 Final submission

The final submission to the JAEA computational benchmark exercise will be carried out on the full geometry without any symmetry or periodic boundary conditions being employed. The results will be calculated section by section based on the division of the test section into sections containing one grid spacer each. The outlet condition of one section will be applied at the inlet of the next. This is done to avoid the production of a prohibitively large mesh.

The final mesh parameters are closely known based on the mesh sensitivity study of Yamagata et al [5] and simulations done for flow through the grid spacer. The 1/3rd full bundle geometry will be used for any final mesh sensitivity tests prior to submission, for the purpose of ensuring sufficient convergence of residuals.

5. Conclusions

A CFD methodology has been developed in preparation for the final submission of computational results to the JAEA computational benchmark exercise. Multiple separate effects studies were summarized and resulted in the choice of SST as the optimal turbulence model to be used for the final submission. SST's failure to adequately predict the turbulent field within a bundle flow has been examined and this failure is expected to be counteracted by the use of a computational mesh that gives increased numerical viscosity.

Future work in an effort to firmly establish Yamagata et al [5] as the proper validation case has been briefly discussed and final results of this study are expected to show this to be true. SST's prediction bias and sensitivity will be further examined prior to final submission. Final results will then be performed on the full bundle geometry and submitted to the JAEA benchmark committee where they will be compared to the results of other researchers who have studied and simulated the same experiment. The results of these comparisons will make up a journal paper to be organized by the JAEA benchmark committee.

6. References

[1] I.L. Pioro and R.B. Duffrey, "Experimental heat transfer in supercritical water flowing inside channels (survey)", Nuclear Engineering and Design, Vol. 235, 2005, pp. 2407-2430.

[2] P.M. Moretti, W.M. Kays, "Heat transfer to a turbulent boundary layer with varying free-stream velocity and varying surface temperature – An experimental study", Int. J. Heat Mass Transfer, Vol. 8, 1965, pp. 1187-1202.

[3] D.P. Mikielewicz, A.M. Shehata, J.D. Jackson, D.M. McEligot, "Temperature, velocity and mean turbulence structure in strongly heated internal gas flows. Comparison of numerical predictions with data", Int. J. Heat Mass Transfer, Vol. 45, No. 21, 2002, pp. 4333-4352.

[4] J.D. Jackson, "Some striking features of heat transfer with fluids at pressures and temperature neat the critical point", Keynote paper for Int. Conf. on Energy Conversion & Application, ICECA, Wuhan, China, 2001.

[5] K. Yamagata, K. Nishikawa, S. Hasegawa, T. Fujii, S. Yoshida, "Forced convective heat transfer to supercritical water flowing in tubes", Int. J. Heat Mass Transfer, Vol. 15, 1972, pp.2575-2593.

[6] F. Roelefs, "CFD analyses of heat transfer to supercritical water flowing vertically upward in a tube", NRG Rep. 21353/04.60811/P, Netherlands Minist. Econ. Aff. http://www.nrg.eu/docs/nrglib/2004/r060811.pdf

[7] S. Koshizuka, N. Takano, Y. Oka, "Numerical analysis of deteriotation phenomena in heat transfer to supercritical water", Int. J. Heat Mass Transfer, Vol. 38, No. 16, 1994, pp.3077-3084.

[8] S. Kim, Y. Kim, Y. Bae, B. Cho, "Numerical simulation of the vertical upward flow of water in a heated tube at supercritical system pressure", Proceedings of ICAPP '04, Pittsburg, PA, United States, 2004.

[9] J. Yang, Y. Oka, Y. Ishiwatari, J. Liu, J. Yoo, "Numerical investigation of heat transfer in upward flows of supercritical water in circular tubes and tight fuel rod bundles", Nuclear Engineering and Design, Vol. 237, 2007, pp. 420-430.

[10] F.R. Menter, "Two-equation eddy-viscosity turbulence models for engineering applications", AAIA Journal, Vol. 32, No. 8, 1994, pp. 1598-1605.

[11] Y. Zhu, "Numerical investigation of the flow and heat transfer within the core cooling channel of a supercritical water reactor", PhD Dissertation, University of Stuttgart, 2010.

[12] V. Yakhot, S.A. Orszag, S. Thangam, T.B. Gatski, C.G. Speziale, "Development of turbulence models for shear flows by a double expansion technique", Physics of Fluids, Vol. 4, 1992, pp. 1510-1520.

[13] D. Palko, H. Anglart, "Theoretical and numerical study of heat transfer deterioration in High Performance Light Water Reactor", Science and Technology of Nuclear Installations, Article ID. 405072, 2008.

[14] A.C. Trupp, R.S. Azad, "The structure of turbulent flow in triangular array rod bundles", Nuclear Engineering and Design, Vol. 32, 1975, pp.47-84.

[15] T. Misawa, T Nakatsuka, H. Yoshida, K. Takase, "Heat transfer experiments and numerical analysis of supercritical pressure water in seven-rod test bundle", Proceedings of NURETH-13, Kanazawa City, Japan, 2009

[16] B. Launder, G. Reece, W. Rodi, "Progress in the development of a Reynolds-stress turbulence closure", Journal of Fluid Mechanics, Vol. 68, Iss. 3, 1975, pp. 537-566.

[17] A. Melling, J. Whitelaw, "Turbulent flow in a rectangular duct", Journal of Fluid Mechanics, Vol. 78, Iss. 2, 1976, pp. 289-315.

[18] A. Demuren, W. Rodi, "Calculation of turbulence-driven secondary motion in non-circular ducts", Journal of Fluid Mechanics, Vol. 140, 1984, pp. 189-222.

[19] K. Seo, "Studies of supercritical heat transfer and flow phenomena", Proceedings of NURETH-11, Avignon, France, 2005